A genetic program for vascular pericyte precursors

Suchit Ahuja[1,2], Cynthia Adjekukor[1,2], Qing Li[1,2], Katrinka M. Kocha[1,2], Nicole Rosin[3], Elodie Labit[3], Sarthak Sinha[3], Ankita Narang[2], Quan Long[1,2], Jeff Biernaskie[2,3], Peng Huang[1,2] and Sarah J. Childs[1,2,*]

1. Department of Biochemistry and Molecular Biology

2. Alberta Children's Hospital Research Institute

3 . Department of Comparative Biology and Experimental Medicine, Faculty of Veterinary Medicine, University of Calgary, Calgary, AB T2N 4N1, Canada.

University of Calgary, 3330 Hospital Drive NW, Calgary AB, T2N 4N1

- Corresponding author: schilds@ucalgary.ca

Abstract

Brain pericytes are critical for regulating endothelial barrier function and activity, thus ensuring adequate blood flow to the brain. The genetic pathways guiding undifferentiated cells into mature pericytes are not well understood. We show here that precursor populations from both neural crest and head mesoderm express the transcription factor *nkx3.1* develop into brain pericytes. We identify the gene signature of these precursors, and show that an *nkx3.1, foxf2a*, and *cxcl12b* -expressing pericyte precursor population is present around the basilar artery prior to artery formation and pericyte recruitment. The precursors later spread throughout the brain and differentiate to express canonical pericyte markers. Cxcl12b- Cxcr4 signaling is required for pericyte attachment and differentiation. Further, both *nkx3.1* and *cxcl12*b are necessary and sufficient in regulating pericyte number as loss inhibits and gain increases pericyte number. Through genetic experiments we have defined a precursor population for brain pericytes and identified genes critical for their differentiation.

Introduction

Endothelial cells and pericytes are key partners in the brain microvessel network. Endothelial cells line the luminal side of vessels, and pericytes attach to the abluminal side of endothelial cells. Pericytes stabilize microvessels by laying extracellular matrix around endothelial cells and regulating vascular tone (1, 2, 3). In addition, pericytes regulate postnatal endothelial sprouting and endothelial morphogenesis via VEGF and TGF-β signaling respectively (2, 4). Consequently, pathologies involving cranial hemorrhage, vessel dilation, and vessel structural defects are common when pericytes are reduced or absent due to loss of key pericyte signalling pathways, Pdgfb (5, 6, 7, 8, 9). Notch activity is also critical for emergence of perivascular mural cells, particularly smooth muscle cells (10, 11, 12). Loss- and gain-of-function of Notch3 receptor in zebrafish revealed a role in brain pericyte proliferation (13). In mice, pericyte loss due to Notch signaling deficiency leads to arteriovenous malformations (14).

Owing to its critical function in vascular homeostasis, pericyte development has received much attention. Quail-chick chimeras showed that pericytes of the forebrain are neural crest derived while aortic pericytes originate from Pax1+ and FoxC2+ sclerotome (15, 16). Mesodermal and neural crest origins of pericytes have also been shown in the zebrafish, where pericytes of the anterior midbrain originate from neural crest and those in the hindbrain and trunk are derived from the paraxial mesoderm (17). Transcriptional and signalling pathways that promote pericyte differentiation include the forkhead box transcription factors FoxC1 and FoxF2 that are required for brain pericyte differentiation and blood-brain barrier maintenance (18, 19). Furthermore, mice and zebrafish lacking FoxC1 and FoxF2 show cerebral hemorrhages (18, 19, 20). In line with this, humans with risk loci near *FOXF2* are more susceptible to stroke and cerebral small vessel disease (21).

While pathways promoting pericyte differentiation have been discovered, the initial signals triggering the convergent differentiation of brain pericyte precursors from two different germ layers are unknown. Here we describe the role of a homeobox transcription factor Nkx3.1, which is required in pericyte precursors originating in both neural crest and paraxial mesoderm. *nkx3.1*$^{-/-}$ mutants exhibit fewer

pericytes, brain hemorrhage, and mispatterned brain vessels. Single cell sequencing on *nkx3.1*-lineage cells reveals that pericyte precursors are marked by the transcription factors *tbx18* and *foxf2a* amongst other genes. Furthermore, we show that chemokine ligand *cxcl12b/sdf1* is expressed in pericyte precursors and functions downstream of *nkx3.1* during pericyte development. Taken together, our study defines a previously unknown pericyte precursor population and a novel Nkx3.1-Cxcl12b cascade during pericyte development.

Results

Brain pericytes originate from a lineage marked by *nkx3.1*

An early marker of the zebrafish sclerotome is the transcription factor, *nkx3.1*. Trunk pericytes are derived from *nkx3.1*-expressing sclerotome precursors, although *nkx3.1* is downregulated when trunk pericytes differentiate (16, 22). Precursor markers for brain pericytes have not yet been identified. Brain pericytes form from two germ layers (neural crest and mesoderm) and an understanding of the convergent genetic program to differentiate cells from different origins into pericytes is also lacking. *nkx3.1* is expressed in the ventral head mesenchyme and trunk of the developing embryo at 16 and 30 hpf, as shown by in situ hybridization (Fig. 1A-B, arrowheads). *nkx3.1* expression in ventral head mesenchyme is still present at 30 hpf but greatly reduced. It is undetectable by 48 hpf (Fig. 1C). Expression of *nkx3.1* occurs far earlier than that of the pericyte marker pdgfrβ, first expressed at 48 hpf in the basilar artery(13). To determine whether brain pericytes originate from *nkx3.1* lineage, we made use of the transgenic lines *TgBAC(nkx3.1:Gal4)*^{ca101} and *Tg(UAS:NTR-mCherry)*^{c264} to raise *nkx3.1:Gal4; UAS:Nitroreductase-mCherry*, hereafter known as *nkx3.1*$^{NTR\text{-}mcherry}$ embryos where *nkx3.1* lineage cells are labelled with mCherry. The mCherry perdures after the native *nkx3.1* mRNA is no longer expressed, allowing us to track cell lineage (22, 23, 24). At 4 days post fertilization (dpf), we observe *nkx3.1*$^{NTR\text{-}mcherry}$ cells in the perivascular zone surrounding endothelial cells (Fig. 1D-E,

arrowheads). These *nkx3.1*-lineage cells show a pericyte-like morphology with a round soma and processes that wrap around endothelial cells (Fig. 1E-F, arrowheads). Furthermore, we found a complete overlap in expression between *nkx3.1*$^{NTR\text{-}mcherry}$ and a transgenic reporter of pericytes, *TgBAC(pdgfrb:GFP)*^{ca41} at 75 hpf (Fig. 1G-I). This confirms that *nkx3.1*$^{NTR\text{-}mcherry}$ perivascular cells in the brain are pericytes at 75 hpf. Since *nkx3.1* is expressed prior to *pdgfrβ*, but their later expression is completely overlapping, this data suggests that *nkx3.1* is expressed in pericyte precursors. To characterize the cellular behavior of *nkx3.1*$^{NTR\text{-}mcherry}$ perivascular cells, we imaged labelled cells in the embryonic brain from 55-65 hpf. Our analysis reveals that *nkx3.1*$^{NTR\text{-}mcherry}$ perivascular cells migrate and proliferate on blood vessels (Fig.1J-M, white and yellow arrowheads; S1 Movie), similar to previously described cellular behavior of pericytes (17).

Previous lineage-tracing data suggests that pericytes in the zebrafish hindbrain originate from mesoderm and that midbrain pericytes originate from neural crest (17). Pericytes in both hindbrain and midbrain express the *nkx3.1* transgene (Fig. 1D). We next used lineage tracing of mesoderm and/or neural crest progenitors to test whether *nkx3.1*-expressing cells arose from one or both germ layers. We used Cre drivers for mesoderm *Tg(tbx6:cre;myl7:GFP)* or neural crest *Tg(sox10:cre;myl7:GFP)* together with a floxed reporter *Tg(loxp-stop-loxp-H2B-GFP*) to lineage label mesodermal or neural crest progeny respectively. We crossed these fish with an *nkx3.1* reporter *TgBAC(nkx3.1:Gal4)*, pericyte reporter *TgBAC(pdgfrb:Gal4FF)* , or endothelial reporter *Tg(kdrl:mCherry)*. This strategy labels cells expressing *pdgfrβ*, *nkx3.1* or *kdrl* in red and mesodermal or neural crest derivatives as green (depending on the experiment). We imaged double positive cells to identify their lineage and observe that both mesoderm and neural crest progenitors contribute to both hindbrain and midbrain pericytes by lineage tracing either pdgfrβ or *nkx3.1* (S1 Fig.).

Taken together, our data shows that *pdgfrβ*-expressing brain pericytes originate from a *nkx3.1* positive precursor, which in turn is generated from *tbx6 and sox10 expressing* mesodermal and neural crest progenitors. *nkx3.1* is therefore a transcription factor expressed in precursors of brain pericytes, but not in mature brain pericytes.

Nkx3.1 function is required for brain pericyte development.

To determine whether Nkx3.1 function is necessary for brain pericyte development, we made an *nkx3.1* mutant zebrafish using CRISPR-Cas9. *nkx3.1*^{ca116} mutants have a 13 bp deletion in exon 2 that is predicted to lead to premature stop prior to the homeobox domain (S2 Fig.). *nkx3.1* $^{-/-}$ mutant embryos show no gross morphological defects. At 75 hpf, we observed no difference in total pericyte number (sum of mid- and hindbrain pericytes) between *nkx3.1*$^{-/-}$ mutants and their heterozygous and wildtype siblings (S3 Fig.), however a previous study showed that *nkx3.1* transcripts are maternally contributed to the developing embryo (25). In order to remove this maternal contribution, we crossed *nkx3.1*$^{+/-}$ males with *nkx3.1*$^{-/-}$ females. Maternal zygotic (MZ) *nkx3.1*$^{-/-}$ embryos show a strong phenotype including brain hemorrhage and hydrocephalus at 52 hpf as compared to controls (Fig. 2A-B). The percentage of MZ *nkx3.1*$^{-/-}$ embryos (27%) exhibiting brain hemorrhage at 52 hpf was significantly higher as compared to *nkx3.1*$^{+/-}$ siblings (12.5%) (Fig. 2C).

Importantly, MZ *nkx3.1*$^{-/-}$ showed significantly fewer pericytes and mispatterned brain vessels at 75 hpf, as observed by confocal microscopy (Fig. 2D-F). This is consistent with the brain hemorrhage phenotype, which is a reported consequence of lack of pericytes (26).

As a second method to test the necessity of *nkx3.1* precursors, we made used the *nkx3.1*$^{NTR\text{-}mcherry}$ transgenic line to ablate *nkx3.1*$^{NTR\text{-}mcherry}$ cells by treating with 5mM metronidazole from 24-48 hpf, a time window during which brain pericyte differentiation is occurring (17). Consistent with the MZ *nkx3.1*$^{-/-}$ phenotype, we observed that the ablation of *nkx3.1*$^{NTR\text{-}mcherry}$ cells resulted in brain hemorrhage at 48 hpf and 72 hpf (S4 Fig.). Furthermore, transgenic embryos treated with metronidazole to induce *nkx3.1*-directed cell ablation showed lack of pericytes and mispatterned brain vasculature at 75 hpf, similar to the *nkx3.1*$^{-/-}$ mutants (S4 Fig.).

To test the sufficiency of Nkx3.1 for pericyte development, we made an *nkx3.1* gain-of-function (GOF) transgenic line *Tg(hsp70l:tBFP-2a-nkx3.1)* expressing Blue fluorescent protein (BFP) fused with

nkx3.1. *Tg(hsp70l:tBFP)* is used as a control. Overexpression of *nkx3.1* using heat shock from 29-30 hpf, when first brain pericytes are emerging, results in more brain pericytes at 75 hpf, compared to overexpression of tBFP alone (Fig. 2G-I). We note that brain vessels of *nkx3.1* GOF embryos appear normal with no gross morphological alteration. Thus *nkx3.1* is both necessary and sufficient for brain pericyte development.

Pericyte precursors share markers with fibroblasts

Although pericytes derive from *tbx6*-positive mesodermal cells and *sox10*-positive neural crest cells, intermediate progenitors have not yet been defined. We have shown that *nkx3.1*-expressing cells differentiate into pericytes and that *nkx3.1* is a marker of pericyte progenitors. Therefore, *nkx3.1* positive cells sampled at a stage prior to pericyte differentiation are a unique population to interrogate the gene expression profile of pericyte precursors. Since not all *nkx3.1* positive cells become brain pericytes (i.e., some become fibroblasts derived from sclerotome cells of the trunk and other lineages), embryos expressing the *nkx3.1*$^{NTR\text{-}mcherry}$ transgene were dissociated from wildtype 30 hpf zebrafish embryos and mCherry-positive FACs sorted cells were subjected to single cell RNA sequencing (scRNAseq; Fig. 3A, B).

We obtained 3359 independent cells for analysis. Using the Uniform Manifold Approximation and Projection algorithm (UMAP) in Seurat (27), we detected thirteen different populations (Fig. 3A, S Table 1). Comparing the top detected genes in each cluster to known markers of lineages, we assigned each cluster to a cell type. 63% of the cells form a group of connected clusters that appear to be progenitors (Prog-1/2) and more differentiated cells. Smaller clusters that have mesoderm and heart, CNS, endothelial, basal fin, CNS or neutrophil properties are also observed, but are not of interest. Of the larger clusters, Prog-2, Fb-V and Fb-A express common fibroblast markers (*col1a1a, col1a1b, pdgfrα, col5a1, mmp2;* S5 Fig) suggesting that this group represents cells differentiating into fibroblast types, potentially including pericyte precursors.

RNA velocity measures transient transcriptional dynamics and infers the differentiation process from an analysis of RNA splicing information in sequencing data. We subclustered the 2120 cells in 5 clusters (Prog-1/2 and Fb-A/B/B). Using RNA velocity, we find that flow direction is consistent with two progenitor pools feeding into the fibroblast clusters, with the Progenitor 1 (Prog-1) cluster feeding into Fb-V and Progenitor 2 (Prog-2) feeding into all 3 clusters (Fb-A, Fb-B and Fb-V; Fig. 3C). Fb-B is a smaller cluster (6% of sorted *nkx3.1* cells) that appears to arise from the Fb-A fibroblast cluster and is likely a more differentiated state.

We identified unique markers in each cluster (Fig. 3D, S6-8 Fig.). Based on genes enriched in the Fb-V cluster, this is most likely a pericyte progenitor cluster. *tbx18* is expressed in the embryonic zebrafish head paraxial mesoderm (28), with enriched expression in adult mouse brain mural cells. A lineage trace of mouse *tbx18* shows expression in both adult mouse pericytes and vascular smooth muscle cells (29, 30). *foxf2* is also enriched in the Fb-V cluster. We have previously shown that *foxf2a* and *foxf2b* are expressed in zebrafish brain pericytes and are essential for generating the proper number of brain pericytes (20, 31). Furthermore, mouse *Foxf2*, is enriched in, and critical for mouse brain pericyte formation (21, 32). A third gene we explore in the Fb-V cluster is *cxcl12b* (Fig. 3N). Vascular mural cells associated with the zebrafish coronary arteries and caudal fin vessels express *cxcl12b* (33, 34). In addition, mural cells of the mouse and human lung tissue express *Cxcl12* (35). These three genes, *tbx18*, *foxf2* and *cxcl12b* strongly argue that Fb-V represent *nkx3.1*-positive pericyte precursors, at a stage prior to when canonical pericyte markers like *pdgfrβ* are expressed, as we have shown that all *nkx3.1*-expressing cells in the brain express pdgfrβ at a later stage (Fig. 1). Canonical pericyte markers like *pdgfrβ, cspg4* and *notch3* are present in scattered cells in these clusters at this time point, but not yet enriched in Fb-V (S9 Fig.*)*. As our data is collected at a stage where there is scant information in other species about the differentiating pericyte gene expression profile and will be very useful for further studies (Supp Table 1).

To validate expression of genes of interest from the Fb-V cluster, we used in situ hybridization at 36 hpf when the first pericytes are associating with developing brain vessels. We find that *tbx18* is

expressed in the perivascular space around the *cxcr4a+* basilar artery (Fig. 3K-M), where the first brain pericytes attach (17). We also detect *foxf2a* and *cxcl12b* expression in *tbx18+* cells (Fig. 3E-J). These data validate single cell sequencing results and confirm the presence of a perivascular cell type that co-expresses *tbx18*, *foxf2a*, and *cxcl12b* around the forming basilar artery, the first site of pericyte attachment (17).

The Fb-A and Fb-B clusters are diverging from Fb-V and express genes reminiscent of sclerotome including *pax9* and *twist2*, while the Fb-B cluster is enriched for fibroblast markers such as *cyr61,* and the *tcf15/paraxis*, involved in trunk mesoderm development. Both clusters express *thrombospondin 4b (thbs4b)*. Since Fb-B flows away from Fb-A, which flows away from Prog-2, this suggests that this lineage is differentiating into traditional fibroblasts that will go on to assume many different lineages, particularly in the zebrafish trunk (23, 24).

Loss of *nkx3.1* leads to transcriptional reduction of the chemokine *cxcl12*

To determine which genes within *nkx3.1*-expressing cells are important for their differentiation, we took advantage of *nkx3.1*^{ca116} genetic mutant fish. At the identical stage to the scRNAseq (30 hpf), we sampled *nkx3.1* wildtype and MZ *nkx3.1* mutant embryos using bulk RNA sequencing. This revealed that 2788 genes were downregulated, and 2080 genes upregulated at 30 hpf (Supplemental table 2, 3). Among the genes downregulated at 30 hpf is *tcf15*, the pericyte marker *ndufa4l2a* and chemokine *cxcl12b* (Fig. 3O). Since we showed that *cxcl12b* is expressed in the pericyte progenitor cluster (Fb-V), we next interrogated the role of Cxcl12b in pericyte development.

Cxcl12b signaling regulates brain pericyte number

Using in situ hybridization at 16 hpf and 24 hpf, we find that *cxcl12b* and *nkx3.1* are co-expressed in the ventral head mesenchyme of the developing embryo (S10 Fig.). We next tested expression of *cxcl12b* in *nkx3.1*$^{-/-}$ mutants. At 30 hpf, *cxcl12b* is strongly downregulated in the head of MZ *nkx3.1*$^{-/-}$

mutants at a location where the first pericytes will attach to the basilar artery (Fig. 4A-C). To test the role of Cxcr4-Cxcl12 signaling in pericyte development, we used AMD 3100, an inhibitor of the Cxcl12 receptor, Cxcr4. The number of brain pericytes is significantly reduced after treatment of zebrafish embryos with 100 µM AMD 3100 from 24-75 hpf (Fig. 4D-F), suggesting requirement of Cxcl12b signaling in pericyte development. In line with this, the mRNA injection of 30 pg *cxcl12b* mRNA not only increases brain pericyte number in wildtype embryos (S11 Fig.) but also rescues brain pericyte number in MZ *nkx3.1*$^{-/-}$ mutants at 75 hpf.

Supporting our results, single-cell sequencing of zebrafish at multiple stages as reported in the DanioCell database(36) shows expression of *nkx3.1, foxf2a* and *cxcl12b* at the 24-34 and 36-48 hpf at a time when *pdgfrβ* is only weakly expressed (S12 Fig.). This independent dataset strongly supports the co-expression of these three genes in the pericyte lineage prior to definitive pericyte marker expression.

Taken together, our data shows that Cxcl12b function is co-expressed with, and required downstream of Nkx3.1 in pericyte development.

Cxcl12b function is required in *nkx3.1*$^{+ve}$ precursors for brain pericyte development

We next tested whether Cxcl12b is required in *nkx3.1*$^{+ve}$ precursors or Pdgfrβ^{+ve} pericytes or in both cell types using a genetic rescue. We created transgenic *cxcl12b* overexpression in *nkx3.1*$^{-/-}$ mutants using *Tg(UAS:cxcl12b;cryaa:mCerulean)*. These fish were crossed with Gal4 drivers in either the *nkx3.1*$^{+ve}$ precursor lineage or Pdgfrβ^{+ve} pericytes using *TgBAC(nkx3.1:Gal4)*^{ca101} or *nkx3.1*$^{-/-}$*;TgBAC(pdgfrb:Gal4FF)*^{ca42}. We scored the number of brain pericytes in mutants carrying both transgenes. We find that *nkx3.1*$^{-/-}$ mutant pericyte numbers are rescued by *nkx3.1*-driven *cxcl12b* overexpression, but not by *cxcl12b* overexpression under a *pdgfrβ* driver at 75 hpf (Fig. 5). Agreeing with the mRNA overexpression data, these experiments confirm the requirement for Cxcl12b in an

early stage of pericyte differentiation in the *nkx3.1* pericyte precursor population but not in later pericyte development (*pdgfrβ*).

Discussion

Little is known about the crucial factors that contribute to the developmental journey of a differentiated pericyte. Most studies focus either on the upstream lineage origins from mesodermal or neural crest precursors, or on downstream genes important for differentiated pericytes but don't address intermediate genetic factors driving lineage differentiation. Here we show that *nkx3.1* is a vital intermediate gene in the differentiation journey of a pericyte. Using a transgenic reporter of *nkx3.1* expression we show that it precedes Pdgfrβ expression in the pericyte lineage. Cells in the brain that express *nkx3.1* become *pdgfrβ*-expressing pericytes. Critically, *nkx3.1* is required for brain pericytes of both mesodermal and neural crest origin, suggesting that it is a gene that unifies the pericyte differentiation program from different lineages. Beyond the brain, previous work shows that *nkx3.1* is in precursors of the trunk pericyte lineage (22), and it is likely that *nkx3.1* is important for pericytes development in other areas of the embryo. We show that the absence of *nkx3.1*-expressing cells results in a severe reduction in pericyte number. Loss of *nkx3.1* and gain of *nkx3.1* show that *nkx3.1* is both necessary and sufficient for modulating brain pericyte number. RNAseq and scRNAseq reveal the transcriptome of *nkx3.1*-expressing pericyte precursors as similar to fibroblasts and identify the chemokine cxcl12 as a critical factor for brain pericyte differentiation, whose expression is controlled by *nkx3.1*.

Brain pericytes are unusual as they arise from two distinct lineages, mesoderm and neural crest in both fish and mouse. No functional differences have been noted between pericytes from different origins. Using lineage tracing, we show that pericytes derived from both paraxial mesoderm (*tbx6*) and neural crest *(sox10*) express *nkx3.1,* and that pericytes derived from both mesoderm and neural crest are present in both the mid brain and hind brain. Previous work has suggested a more compartmentalized contribution in fish where mesoderm contributes to hind brain pericytes and neural

crest contributes to mid brain pericytes (17). This may have occurred due to incomplete sampling in these difficult experiments, as similar reagents were used. The rarity of recombination events limits precise quantification of mesodermal and neural crest contribution, but contributions from both mesodermal (myeloid) and neural crest lineages to brain pericytes is also observed in mice (37).

Ablation of *nkx3.1* expressing cells or loss of the *nkx3.1* gene within these cells leads to an identical phenotype. Loss of *nkx3.1*-expressing cells or of *nkx3.1* leads to typical hallmarks of pericyte disruption including brain hemorrhage, reduced pericyte number and, mispatterned brain vessels, suggesting a critical role of Nkx3.1 in brain pericyte development. The level of pericyte loss is similar to that reported for both *foxf2* and *notch3* knockout fish suggesting that all three genes key players in pericyte differentiation (13, 20). We show that gain of Nkx3.1 leads to an increase in pericyte number. The only other gene that is sufficient to increase pericyte number is *notch3,* suggesting that Nkx3.1 and Notch3 may potentially act using similar downstream mechanisms (13).

Where and when *nkx3.1* acts in the pericyte differentiation cascade is an important question. We note that *nkx3.1* is an early embryonic gene and by 48 hpf its mRNA is undetectable, however perdurance of the *nkx3.1*$^{NTR\text{-}mcherry}$ transgenic allowed us to follow cells after the endogenous gene has turned off. Nothing is known of the Nkx3.1 protein and how long it may remain in an embryo, however, our data point to a specific early role in development. Incidentally, the first brain pericytes attach to the basilar artery by 36 hpf, and *nkx3.1* is expressed before this time.

To define the gene signature of this pericyte precursor population before pericyte markers are observed, we used single cell sequencing of sorted *nkx3.1*$^{NTR\text{-}mCherry}$ cells at 30 hpf. Analysis of single cells revealed *nkx3.1* contribution in thirteen gene clusters, of which the majority of *nkx3.1* positive cells belong to two precursor clusters and three fibroblast-like clusters as defined by expression of pan-fibroblast markers such as *col1a1, col5a1* and *pdgfrα* (Fig S5) (32). Interestingly, one cluster Fb-V was found to be enriched in genes reported in pericytes and/or crucial for their development, i.e., *tbx18* (30, 38), *cxcl12b* (33, 34, 35), and *foxf2a* (19, 20, 21). However, the Fb-V cluster lacks expression of ‘classical’ differentiated pericyte markers, including *Pdgfrβ (17)*, *abcc9 (12, 39)*, *Kcnj8*

(39), *ndufa4l2a and kcne4 (40)*, which indicates that Fb-V are fibroblast-like precursors and not differentiated cells, which are observed three days later in development. Of the two precursor clusters, Prog1 has extremely high expression of ribosomal protein subunits (30 *rps* (small ribosome) and 44 *rpl* (large ribosome) genes). Expression of *rps* and *rpl* genes is very enriched in mural cells from early human development (GW15-18) in comparison to later development (GW20-23) (41), suggesting that this cluster represents early precursors. The second precursor cluster, Prog2, overlaps in expression profile with all three fibroblast clusters (A, B, V). RNA velocity analysis suggest that Prog1 contributes to Fb-V and CNS *nkx3.1*-expressing derivatives, while Prog2 contributes to mesoderm (including heart mesoderm), Fb-V and the two sclerotome fibroblast clusters Fb-A and Fb-B. RNA velocity also suggests that FB-V is differentiating from Fb-A, and that Fb-B is further differentiated from Fb-A. These two fibroblast clusters express classical markers of sclerotome, an expected major population of *nkx3.1*-expressing cells (22). Although it has a similar gene expression profile, sclerotome is spatially separate from brain pericytes in the embryo and forms the trunk mesenchyme. Extensive characterization of the pericyte transcriptome by scRNAseq in the adult mouse, differentiated fish pericyte (5 dpf), and embryonic human are all from later developmental stages than the transcriptome that we determine here, and therefore not completely overlapping (40, 41, 42).

To understand functional targets of Nkx3.1 in pericyte differentiation, we undertook bulk RNA sequencing of *nkx3.1* mutants at 30 hpf. Among the downregulated genes, we found *ndufa4l2a* (a pericyte marker) (40), and *cxcl12b* are both downregulated in *nkx3.1*$^{-/-}$ embryos at 30 hpf. This is intriguing as single cell RNA sequencing showed expression of chemokine *cxcl12b* in *nkx3.1*-expressing fibroblasts, including Fb-V, and Cxcl12-cxcr4 signalling is involved in bone marrow-derived pericyte differentiation (43) and Cxcl12 also plays a role in recruitment of vascular smooth muscle cells to the zebrafish aorta (44), thus it is a strong candidate. We show that *nkx3.1* positive pericyte precursors co-express *cxcl12b*, *tbx18, and foxf2a,* confirming our single cell RNA sequencing data. Functional inhibition of Cxcl12-Cxcr4 signaling through a small molecule Cxcr4 inhibitor significantly

reduced pericyte numbers in wild type larvae, demonstrating a role for the pathway in pericyte differentiation. We next demonstrated that *cxcl12b* is a key downstream effector in *nkx3.1*-positive pericyte precursors through genetic rescue, either under promoters for *nkx3.1* (early precursors) or *pdgfrb* (more mature pericytes). Tellingly, *cxcl12b* overexpression was only able to rescue pericyte numbers in *nkx3.1* mutants when expressed early, but not once pericytes had differentiated to express *pdgfrb*. Taken together, this suggests that expression of *nkx3.1* in a pericyte precursor promotes the expression of the chemokine *cxcl12* and influences pericyte differentiation). As a model, Cxcl12 released by pericyte precursors would likely interact with Cxcr4a, known to be expressed on the proximal basilar artery. Based on the model for smooth muscle cell recruitment (44), endothelial cells in turn might produce the Pdgfb ligand to facilitate attachment of Pdgfrβ+ pericytes on the basilar artery (45). Previous work suggesting that Pdgfb is attenuated with Cxcl12-Cxcr4 signalling inhibition supports our hypothesis (43).

Our study identifies a new player in pericyte differentiation, the transcription factor, *nkx3.1*. *nkx3.1* is required in an intermediate precursor cell state that exists temporally downstream of germ layer (mesoderm or neural crest) specification, and upstream of differentiated pericytes expressing canonical makers. The role of *nkx3.1* in brain pericyte precursors is transient and is in parallel to its role in trunk sclerotome, although these are distinct cells. We identify the key role of nkx3.1 in promoting the proper number of pericytes to emerge on brain vessels to promote downstream vascular stability. We show that expression of *nkx3.1* is necessary and sufficient to modulate developmental pericyte number. Nkx3.1 modulates pericyte number through promotion of chemokine ligand Cxcl12b expression, a second gene that we demonstrate is necessary and sufficient for developmental brain pericyte number. We define the novel gene expression signature of *nkx3.1*-expressing pericyte precursors using scRNAseq, which opens new avenues for understanding pericyte differentiation. For instance, expression of two transcription factors in the Fb-V cluster (*foxf2a, tbx18*) are associated with pericytes in previous studies (20, 21, 29, 30), but with poorly described roles, although regulatory changes in FOXF2 are associated with stroke in humans (20, 46). Future work focusing on additional intermediate genes in pericyte differentiation will be critical for

understanding the stepwise differentiation of pericytes from upstream precursors, and potential for regeneration in disease where pericytes are lost.

Data availability

Bulk and single-cell RNA-Sequencing data reported in this work are available through NCBI GEO (GSE232763, private token: ohclkugmhnkjlwd).

Methods

Zebrafish: All procedures were conducted in compliance with the Canadian Council on Animal Care, and ethical approval was granted by the University of Calgary Animal Care Committee (AC21-0189). All experiments included wildtype or vehicle-treated controls as a comparison group and developmental stages, n's, genotypes, and statistical outcomes are noted for each experiment. Embryos were maintained in E3 medium at 28C. For heat shock experiments, embryos were heated for 1 hour at 39C in a heating block.

The following published strains were used: *TgBAC(nkx3.1:Gal4)*^{ca101} *(23)*, *Tg(UAS:NTR-mCherry)*^{c264} (47), *Tg(kdrl:GFP)*^{la116} (48), *TgBAC(pdgfrβ:GFP)*^{ca41} (3), *TgBAC(pdgfrβ:Gal4)*^{ca42} (3), *Tg(kdrl:mCherry)*^{ci5} (49).

The following strains were generated for this manuscript: *Tg(hsp70l:tBFP)*^{ca90}, *Tg(hsp70l:tBFP-2a-nkx3.1)*^{ca91} .First, middle entry clones of tagBFP (Evrogen), tagBFP PCR-fused to *nkx3.1* or *cxcl12b* were made by amplification using primers are in S3 Table and cloning into pDONR221 using BP Clonase (ThermoFisher). Transposon Tol2 vectors were assembled using LR Clonase (ThermoFisher) and the Tol2 vector (50). *Tg(tbx6:cre;myl7:GFP)*^{ca92} and *Tg(sox10:cre;myl7:GFP)*^{ca93} were injected in our laboratory from Tol2 plasmids provided by Tom Carney (51). *Tg(*hsp70l-loxP-STOP-loxP-H2B-GFP_cryaa-cerulean)^{ca94} was created from Addgene plasmid 24334 (52) by digestion with XhoI and re-ligation. This deleted mCherry but maintains the stop sequences and was followed by injection into zebrafish and raising of F1 and further generations from the F0 founder.

The *nkx3.1*^{ca116} mutant was generated using CRISPR/Cas9 as previously described(53). Target sites were identified using CHOPCHOP (54). The guide sequence was 5'-GGGGAGGCGGGAAAAAGAAGCGG -3' . To assemble DNA templates for sgRNA transcription, gene-specific oligonucleotides containing the T7 promoter sequence (5'-TAATACGACTCACTATA-3'), the 20-base target site, and a complementary sequence were annealed to a constant oligonucleotide encoding the reverse-complement of the tracrRNA tail. sgRNAs were generated by in vitro transcription using the Megascript kit (Ambion). Cas9 mRNA was transcribed from linearized pCS2-Cas9 plasmid using the mMachine SP6 kit (Ambion). To generate mutants, one-cell stage wild-type embryos were injected with a mix containing 20 ng/µl sgRNA and 200 ng/µl Cas9 mRNA. Injected fish were raised to adulthood and crossed to generate F1 embryos. T7 Endonuclease I assay (NEB) was then used to identify the presence of indel mutations in the targeted region of F1 fish. *nkx3.1*^{ca116} has a 13 bp deletion (S2 Fig.).

In situ hybridization: For Hybridization Chain Reaction (HCR) in situ hybridization, custom probes for *nkx3.1, tbx18, foxf2a*, *cxcr4a* and *cxcl12b* were obtained from Molecular Instruments (Los Angeles, CA). The in-situ staining reactions occurred as recommended by the manufacturer.

Microscopy: Embryos were imaged with a 20x objective on an inverted Zeiss LSM880 Airyscan or LSM900 laser confocal microscope while mounted in low-melt agarose.

Statistical analysis used GraphPad Prism 7 software, using a one-way ANOVA with multiple comparisons and a Tukey's or Dunnett's post-hoc test. Results are expressed as mean ± SD. The N's of biological and n's of technical replicates, p-values and statistical test used are provided in the figure legends.

Drug treatments: All small molecules are listed in S4 Table.

Embryo dissociation and FACs sorting

~500 wildtype 30 hpf zebrafish embryos on the TL background expressing the *Tg(nkx3.1:Gal4;UAS:NTR-mCherry)*^{ca101} transgene (22) were anesthetized in Tricaine, kept on ice, and then dissociated with 0.25% Trypsin in 1mM EDTA at 28C with 300 rpm shaking for 20 minutes. The reaction was stopped using 1.25 µL 0.8M $CaCl_2$ and 100 µL 1% FBS. Cells were washed in 1%FBS in Dulbecco's PBS 3 times before straining through 75 µm and 30 µm strainers (Greiner Bio-One and Miltenyi Biotec) in Dulbecco's PBS. Cell viability was determined using Trypan blue (Sigma) and was greater than 80%. Cells were subjected to FACS (BD Facs Aria III, BD Biosciences) sorting for mCherry and excluding doublets and non-viable cells.

scRNA-Seq library construction, sequencing and analysis

Two independent libraries were generated from FACS-sorted *nkx3.1* expressing cells using the Chromium Single Cell Chip A kit, and the Chromium Single cell 3′ Library & Gel beaded kit V3 and 3.1 Next GEM (10x Genomics; Pleasanton, CA, USA). Libraries were sequenced on the Illumina NovaSeq using an S2 Flowcell (Illumina) at the Centre for Health Genomics and Informatics, University of Calgary. All raw FASTQs were aligned to the zebrafish reference genome GRCz11 (version 4.3.2) generated using Cellranger version 3.1.0 mkref pipeline. The gene-barcode matrix output was processed using Seurat v3 pipeline in R (55). Quality control steps filtered out cells expressing fewer than 200 genes or more than 2500 genes, as well as cells that had a mitochondrial content <5%. A total of 3359 cells was used for analysis. Uniform manifold approximation and projection (UMAP) with 15 principal components and resolution of 0.6 was used for dimension reduction. Cell clusters were assigned based on known gene expression in cell lineages.

RNA velocity pipeline for Seurat objects (Satija lab) was implemented to perform RNA velocity analysis. Loom files were generated from position-sorted aligned BAM files using velocyto (version-0.17.15) (56).A combined loom file containing counts of spliced, unspliced and ambiguous transcripts of both samples was read using Seurat function ReadVelocity. Count table of spliced and unspliced transcripts (stored as Seurat object) was processed to merge with existing Seurat object generated for

cluster identification. Velocity analysis was performed on the integrated Seurat object using velocyto.R (56). RNA velocity vectors were projected on UMAP embeddings generated during cluster generation.

Bulk RNA sequencing:

30 hpf MZ *nkx3.1*^{ca116} mutant and wild type embryos were collected and RNA prepared using Trizol (ThermoFisher, Waltham MA). Libraries were prepared from 50ng/µg/µl of total mRNA per sample using the Illumina Ultra II directional RNA library prep (SanDiego, CA), and sequenced via the NovaSeq SP 100 cycle v 1.5 sequencing run with 33 million reads per sample. 4 replicates were sequenced per condition.

For bulk RNASeq, quality control evaluations performed by FastQC v0.11.9 (57) revealed that the reads were of high quality and required no trimming step. Consequently, the reads were mapped to the reference genome danRer11 obtained from UCSC and gene annotation file Zebrafish ENSEMBL Lawson v4.3.2 (58) using the splice-aware alignment tool, STAR v2.7.8a (59). STAR was run on default settings with the additional optional command '--quantMode GeneCounts' to generate the gene counts files. The gene counts files were filtered for genes with less than 10 counts and normalized to the median ratio using DESeq2 v1.34.0 (60). Differentially expressed genes were identified as genes with FDR-adjusted p-value < 0.05 and log2(fold-change) < -0.5 or log2(foldchange) > 0.5. Volcano plots of differentially expressed genes was generated using Enhanced Volcano v1.12.0 (61).

S1 Table. 30 hpf scRNAseq (see Excel sheet)

S2 Table. 30 hpf bulk RNAseq (see Excel sheet)

S3 Table: Primers, guides, HCR probes

Name	Sequence
Nkx3.1-gtp-f	cacagATTCAGCGGATACTTGTCG
Nkx3.1-gtp-r	aatacCTGCAGGTGCGTGAA
Nkx3.1 guide	GGGGAGGCGGGAAAAAGAAGCGG
UAS_Cxcl12bFw	GGGGACAAGTTTGTACAAAAAAGCAGGCTGCCACCATGGATAG CAAAGTAGTAGCG
UAS_Cxcl12bRv	GGGGACCACTTTGTACAAGAAAGCTGGGTTTACTCTGAGCGTT TCTTCTTT
attb1-Kozak-BFP F	GGGGACAAGTTTGTACAAAAAAGCAGGCTTCACCATGGTGTCT AAAGGAGAG
2A-BFP R	AGGACCAGGATTTTCTTCAACATCACCAGCTTGTTTTAATAAAG AAAAATTAGTAGCACCAGAACCATTCAGCTTGTGTCCCAGTT
2A-nkx3.1 F	GCTGGTGATGTTGAAGAAAATCCTGGTCCTAGTCGAGCTGTGC AGAGTGA
attb2-nkx3.1 R	GGGGACCACTTTGTACAAGAAAGCTGGGTTTCACAGTGCTGGT CTCCACA
Nkx3.1 HCR probe	Molecular Instruments
Cxcl12b HCR probe	Molecular Instruments
Tbx18 HCR probe	Molecular Instruments
FoxF2a HCR probe	Molecular Instruments

S4 Table: Reagent Table

Chemical name	Source	Catalog number	Concentration
Metronidazole	Sigma	M3761	5mM
AMD 3100	Sigma	A5602	100 µM
Chromium Single Cell Chip A kit	10X Genomics	120236	
Chromium Next GEM Single Cell 3' GEM, Library & Gel Bead Kit v3.1	10X Genomics	1000075/ 1000128	

References

1. Stratman AN, Malotte KM, Mahan RD, Davis MJ, Davis GE. Pericyte recruitment during vasculogenic tube assembly stimulates endothelial basement membrane matrix formation. Blood. 2009;114(24):5091-101.
2. Dave JM, Mirabella T, Weatherbee SD, Greif DM. Pericyte ALK5/TIMP3 Axis Contributes to Endothelial Morphogenesis in the Developing Brain. Dev Cell. 2018;47(3):388-9.
3. Bahrami N, Childs SJ. Development of vascular regulation in the zebrafish embryo. Development. 2020;147(10).
4. Eilken HM, Dieguez-Hurtado R, Schmidt I, Nakayama M, Jeong HW, Arf H, et al. Pericytes regulate VEGF-induced endothelial sprouting through VEGFR1. Nat Commun. 2017;8(1):1574.
5. Soriano P. Abnormal kidney development and hematological disorders in PDGF beta-receptor mutant mice. Genes Dev. 1994;8(16):1888-96.
6. Hellstrom M, Kalen M, Lindahl P, Abramsson A, Betsholtz C. Role of PDGF-B and PDGFR-beta in recruitment of vascular smooth muscle cells and pericytes during embryonic blood vessel formation in the mouse. Development. 1999;126(14):3047-55.
7. Lindahl P, Johansson BR, Leveen P, Betsholtz C. Pericyte loss and microaneurysm formation in PDGF-B-deficient mice. Science. 1997;277(5323):242-5.
8. Leveen P, Pekny M, Gebre-Medhin S, Swolin B, Larsson E, Betsholtz C. Mice deficient for PDGF B show renal, cardiovascular, and hematological abnormalities. Genes Dev. 1994;8(16):1875-87.
9. Ando K, Shih YH, Ebarasi L, Grosse A, Portman D, Chiba A, et al. Conserved and context-dependent roles for pdgfrb signaling during zebrafish vascular mural cell development. Dev Biol. 2021;479:11-22.
10. Joutel A. Pathogenesis of CADASIL: transgenic and knock-out mice to probe function and dysfunction of the mutated gene, Notch3, in the cerebrovasculature. Bioessays. 2011;33(1):73-80.
11. Kofler NM, Cuervo H, Uh MK, Murtomäki A, Kitajewski J. Combined deficiency of Notch1 and Notch3 causes pericyte dysfunction, models CADASIL, and results in arteriovenous malformations. Sci Rep. 2015;5:16449.
12. Ando K, Wang W, Peng D, Chiba A, Lagendijk AK, Barske L, et al. Peri-arterial specification of vascular mural cells from naive mesenchyme requires Notch signaling. Development. 2019;146(2).
13. Wang Y, Pan L, Moens CB, Appel B. Notch3 establishes brain vascular integrity by regulating pericyte number. Development. 2014;141(2):307-17.
14. Henshall TL, Keller A, He L, Johansson BR, Wallgard E, Raschperger E, et al. Notch3 is necessary for blood vessel integrity in the central nervous system. Arterioscler Thromb Vasc Biol. 2015;35(2):409-20.
15. Etchevers HC, Vincent C, Le Douarin NM, Couly GF. The cephalic neural crest provides pericytes and smooth muscle cells to all blood vessels of the face and forebrain. Development. 2001;128(7):1059-68.
16. Pouget C, Pottin K, Jaffredo T. Sclerotomal origin of vascular smooth muscle cells and pericytes in the embryo. Dev Biol. 2008;315(2):437-47.
17. Ando K, Fukuhara S, Izumi N, Nakajima H, Fukui H, Kelsh RN, et al. Clarification of mural cell coverage of vascular endothelial cells by live imaging of zebrafish. Development. 2016;143(8):1328-39.
18. Siegenthaler JA, Choe Y, Patterson KP, Hsieh I, Li D, Jaminet SC, et al. Foxc1 is required by pericytes during fetal brain angiogenesis. Biol Open. 2013;2(7):647-59.
19. Reyahi A, Nik AM, Ghiami M, Gritli-Linde A, Ponten F, Johansson BR, et al. Foxf2 Is Required for Brain Pericyte Differentiation and Development and Maintenance of the Blood-Brain Barrier. Dev Cell. 2015;34(1):19-32.
20. Ryu JR, Ahuja S, Arnold CR, Potts KG, Mishra A, Yang Q, et al. Stroke-associated intergenic variants modulate a human FOXF2 transcriptional enhancer. Proc Natl Acad Sci U S A. 2022;119(35):e2121333119.
21. Neurology Working Group of the Cohorts for H, Aging Research in Genomic Epidemiology Consortium tSGN, the International Stroke Genetics C. Identification of additional risk loci for stroke and small vessel disease: a meta-analysis of genome-wide association studies. Lancet Neurol. 2016;15(7):695-707.
22. Rajan AM, Ma RC, Kocha KM, Zhang DJ, Huang P. Dual function of perivascular fibroblasts in vascular stabilization in zebrafish. PLoS Genet. 2020;16(10):e1008800.

23. Ma RC, Jacobs CT, Sharma P, Kocha KM, Huang P. Stereotypic generation of axial tenocytes from bipartite sclerotome domains in zebrafish. PLoS Genet. 2018;14(11):e1007775.
24. Ma RC, Kocha KM, Méndez-Olivos EE, Ruel TD, Huang P. Origin and diversification of fibroblasts from the sclerotome in zebrafish. Dev Biol. 2023;498:35-48.
25. Rauwerda H, Wackers P, Pagano JF, de Jong M, Ensink W, Dekker R, et al. Mother-Specific Signature in the Maternal Transcriptome Composition of Mature, Unfertilized Zebrafish Eggs. PLoS One. 2016;11(1):e0147151.
26. Nadeem T, Bogue W, Bigit B, Cuervo H. Deficiency of Notch signaling in pericytes results in arteriovenous malformations. JCI Insight. 2020;5(21).
27. Hao Y, Hao S, Andersen-Nissen E, Mauck WM, 3rd, Zheng S, Butler A, et al. Integrated analysis of multimodal single-cell data. Cell. 2021;184(13):3573-87.e29.
28. Begemann G, Gibert Y, Meyer A, Ingham PW. Cloning of zebrafish T-box genes tbx15 and tbx18 and their expression during embryonic development. Mech Dev. 2002;114(1-2):137-41.
29. He L, Vanlandewijck M, Raschperger E, Andaloussi Mae M, Jung B, Lebouvier T, et al. Analysis of the brain mural cell transcriptome. Sci Rep. 2016;6:35108.
30. Guimaraes-Camboa N, Cattaneo P, Sun Y, Moore-Morris T, Gu Y, Dalton ND, et al. Pericytes of Multiple Organs Do Not Behave as Mesenchymal Stem Cells In Vivo. Cell Stem Cell. 2017;20(3):345-59 e5.
31. Chauhan G, Arnold CR, Chu AY, Fornage M, Reyahi A, Bis JC, et al. Identification of additional risk loci for stroke and small vessel disease: a meta-analysis of genome-wide association studies. The Lancet Neurology. 2016;Jun 15 (7):695-707.
32. Muhl L, Genove G, Leptidis S, Liu J, He L, Mocci G, et al. Single-cell analysis uncovers fibroblast heterogeneity and criteria for fibroblast and mural cell identification and discrimination. Nat Commun. 2020;11(1):3953.
33. Kapuria S, Bai H, Fierros J, Huang Y, Ma F, Yoshida T, et al. Heterogeneous pdgfrb+ cells regulate coronary vessel development and revascularization during heart regeneration. Development. 2022;149(4).
34. Lund TC, Patrinostro X, Kramer AC, Stadem P, Higgins LA, Markowski TW, et al. sdf1 Expression reveals a source of perivascular-derived mesenchymal stem cells in zebrafish. Stem Cells. 2014;32(10):2767-79.
35. Yuan K, Liu Y, Zhang Y, Nathan A, Tian W, Yu J, et al. Mural Cell SDF1 Signaling Is Associated with the Pathogenesis of Pulmonary Arterial Hypertension. Am J Respir Cell Mol Biol. 2020;62(6):747-59.
36. Sur A, Wang Y, Capar P, . GM, Farrell JA. Single-cell analysis of shared signatures and transcriptional diversity during zebrafish development. bioRxiv. 2023.
37. Yamazaki T, Nalbandian A, Uchida Y, Li W, Arnold TD, Kubota Y, et al. Tissue Myeloid Progenitors Differentiate into Pericytes through TGF-beta Signaling in Developing Skin Vasculature. Cell Rep. 2017;18(12):2991-3004.
38. Xu J, Nie X, Cai X, Cai CL, Xu PX. Tbx18 is essential for normal development of vasculature network and glomerular mesangium in the mammalian kidney. Dev Biol. 2014;391(1):17-31.
39. Ando K, Tong L, Peng D, Vazquez-Liebanas E, Chiyoda H, He L, et al. KCNJ8/ABCC9-containing K-ATP channel modulates brain vascular smooth muscle development and neurovascular coupling. Dev Cell. 2022;57(11):1383-99 e7.
40. Shih YH, Portman D, Idrizi F, Grosse A, Lawson ND. Integrated molecular analysis identifies a conserved pericyte gene signature in zebrafish. Development. 2021;148(23).
41. Crouch EE, Bhaduri A, Andrews MG, Cebrian-Silla A, Diafos LN, Birrueta JO, et al. Ensembles of endothelial and mural cells promote angiogenesis in prenatal human brain. Cell. 2022;185(20):3753-69 e18.
42. Vanlandewijck M, He L, Mae MA, Andrae J, Ando K, Del Gaudio F, et al. A molecular atlas of cell types and zonation in the brain vasculature. Nature. 2018;554(7693):475-80.
43. Hamdan R, Zhou Z, Kleinerman ES. Blocking SDF-1alpha/CXCR4 downregulates PDGF-B and inhibits bone marrow-derived pericyte differentiation and tumor vascular expansion in Ewing tumors. Mol Cancer Ther. 2014;13(2):483-91.
44. Stratman AN, Burns MC, Farrelly OM, Davis AE, Li W, Pham VN, et al. Chemokine mediated signalling within arteries promotes vascular smooth muscle cell recruitment. Commun Biol. 2020;3(1):734.

45. Betsholtz C. Insight into the physiological functions of PDGF through genetic studies in mice. Cytokine Growth Factor Rev. 2004;15(4):215-28.
46. Chauhan G. Identification of additional risk loci for stroke and small vessel disease: a meta-analysis of genome-wide association studies. Lancet Neurol. 2016;15(7):695-707.
47. Davison JM, Akitake CM, Goll MG, Rhee JM, Gosse N, Baier H, et al. Transactivation from Gal4-VP16 transgenic insertions for tissue-specific cell labeling and ablation in zebrafish. Dev Biol. 2007;304(2):811-24.
48. Choi J, Mouillesseaux K, Wang Z, Fiji HD, Kinderman SS, Otto GW, et al. Aplexone targets the HMG-CoA reductase pathway and differentially regulates arteriovenous angiogenesis. Development. 2011;138(6):1173-81.
49. Proulx K, Lu A, Sumanas S. Cranial vasculature in zebrafish forms by angioblast cluster-derived angiogenesis. Dev Biol. 2010;348(1):34-46.
50. Kwan KM, Fujimoto E, Grabher C, Mangum BD, Hardy ME, Campbell DS, et al. The Tol2kit: a multisite gateway-based construction kit for Tol2 transposon transgenesis constructs. Dev Dyn. 2007;236(11):3088-99.
51. Lee RT, Knapik EW, Thiery JP, Carney TJ. An exclusively mesodermal origin of fin mesenchyme demonstrates that zebrafish trunk neural crest does not generate ectomesenchyme. Development. 2013;140(14):2923-32.
52. Hesselson D, Anderson RM, Beinat M, Stainier DY. Distinct populations of quiescent and proliferative pancreatic beta-cells identified by HOTcre mediated labeling. Proc Natl Acad Sci U S A. 2009;106(35):14896-901.
53. Gagnon JA, Valen E, Thyme SB, Huang P, Akhmetova L, Pauli A, et al. Efficient mutagenesis by Cas9 protein-mediated oligonucleotide insertion and large-scale assessment of single-guide RNAs. PLoS One. 2014;9(5):e98186.
54. Labun K, Montague TG, Gagnon JA, Thyme SB, Valen E. CHOPCHOP v2: a web tool for the next generation of CRISPR genome engineering. Nucleic Acids Res. 2016;44(W1):W272-6.
55. Stuart T, Butler A, Hoffman P, Hafemeister C, Papalexi E, Mauck WM, 3rd, et al. Comprehensive Integration of Single-Cell Data. Cell. 2019;177(7):1888-902.e21.
56. La Manno G, Soldatov R, Zeisel A, Braun E, Hochgerner H, Petukhov V, et al. RNA velocity of single cells. Nature. 2018;560(7719):494-8.
57. Andrews S. FastQC: A Quality Control Tool for High Throughput Sequence Data. 2010.
58. Lawson ND, Li R, Shin M, Grosse A, Yukselen O, Stone OA, et al. An improved zebrafish transcriptome annotation for sensitive and comprehensive detection of cell type-specific genes. Elife. 2020;9.
59. Dobin A, Davis CA, Schlesinger F, Drenkow J, Zaleski C, Jha S, et al. STAR: ultrafast universal RNA-seq aligner. Bioinformatics. 2013;29(1):15-21.
60. Love MI, Huber W, Anders S. Moderated estimation of fold change and dispersion for RNA-seq data with DESeq2. Genome Biol. 2014;15(12):550.
61. Blighe K, Rana, S., Lewis, M. EnhancedVolcano: Publication-ready volcano plots with enhanced colouring and labeling. R package version 1. 2018.

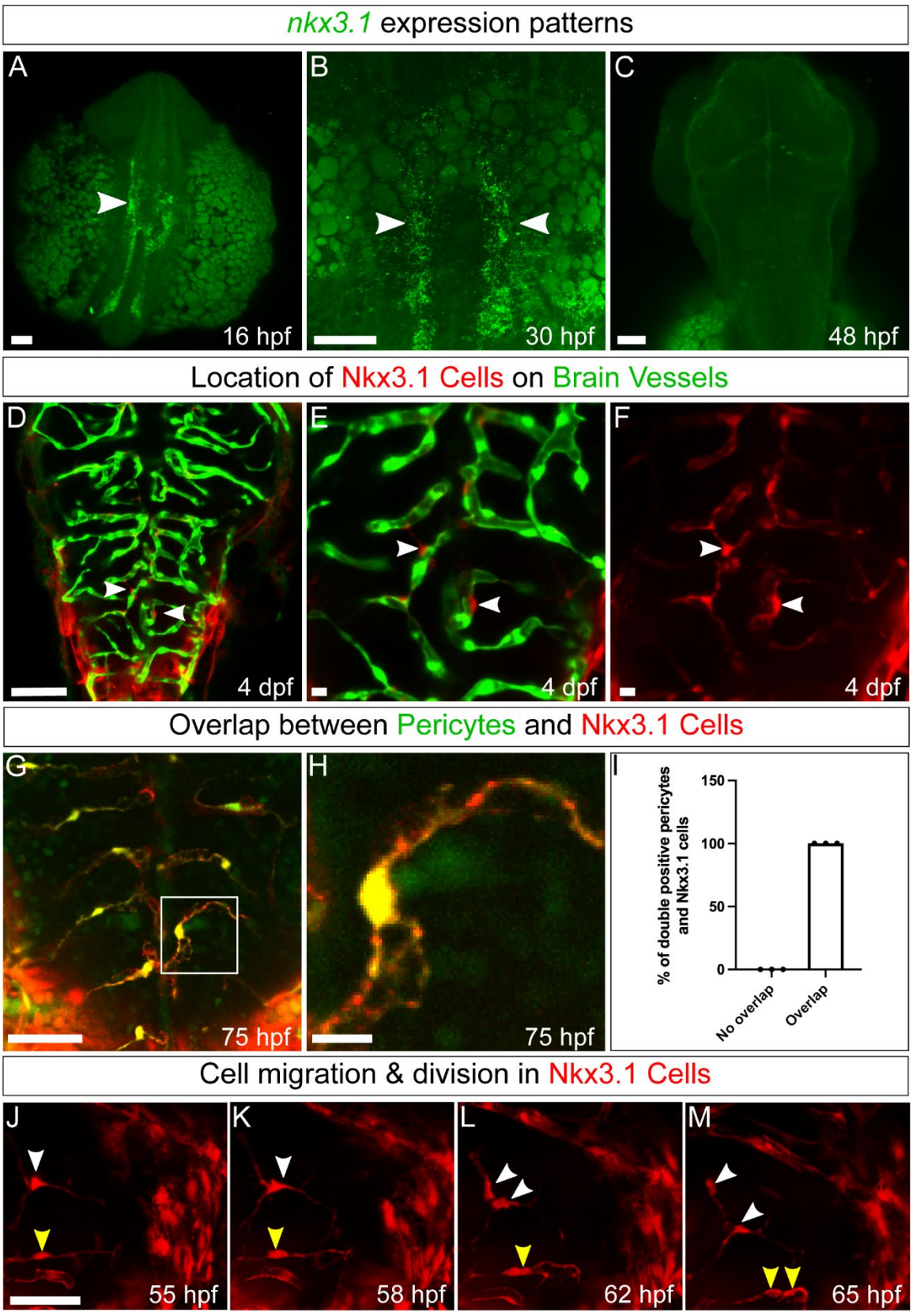

Fig. 1: *nkx3.1* expression patterns and cell behavior. All images are captured dorsally. (A-C) Expression of *nkx3.1* by HCR in situ hybridization. (A) At 16 hpf, *nkx3.1* is expressed in the hindbrain and anterior trunk. Arrowheads mark *nkx3.1* expression. (B) At 30 hpf, *nkx3.1* is expressed in the posterior head and trunk. (C) At 48 hpf, *nkx3.1* expression is not detectable. (D, E) *nkx3.1*$^{NTR\text{-}mcherry}$ cells (red) are adjacent to endothelium (green; *Tg(flk:GFP)*) in brain vessels at 4 dpf. (F) Single channel image of *nkx3.1*$^{NTR\text{-}mcherry}$ cells showing cellular processes. Arrowheads in D, E, and F mark same *nkx3.1*$^{NTR\text{-}mcherry}$ perivascular cells. (G) Brain pericytes labelled by *TgBAC(pdgfrβ:GFP)* coexpress *nkx3.1*$^{NTR\text{-}mcherry}$ 75 hpf. (H) Enlargement of an individual brain pericyte marked by a square in G. (I) Quantification brain pericytes co-expressing Nkx3.1 at 75 hpf (N=3 experiments and 30 embryos). (J-M) Single images from timelapse of *nkx3.1*$^{NTR\text{-}mcherry}$ cells in the midbrain. White and yellow arrowheads track individual cells that migrate and divide with time. Scale bar in all images is 50μm.

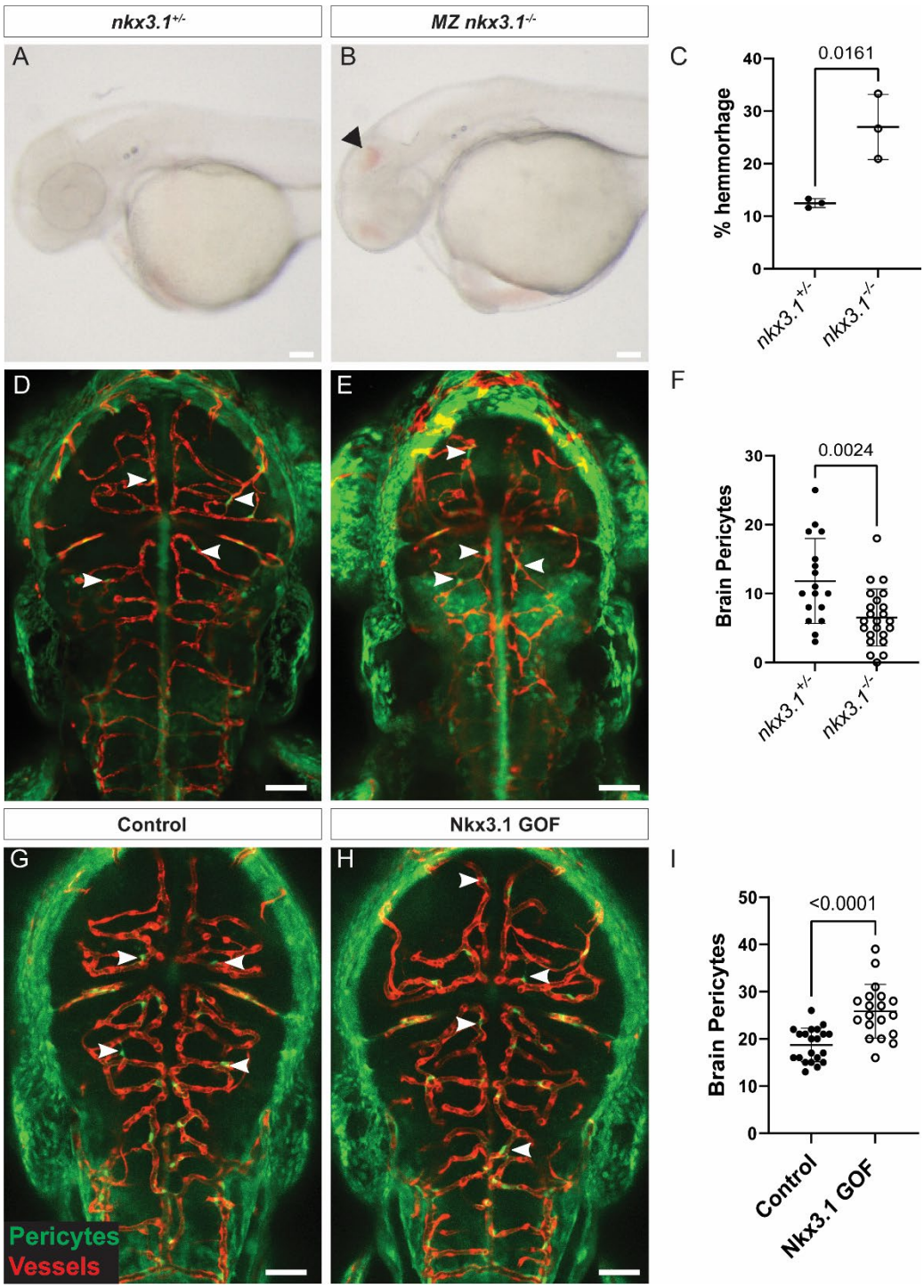

Fig. 2: Nkx3.1 function is required to regulate brain pericyte numbers. (A-C) Lateral view of *nkx3.1*$^{-/-}$ MZ mutants showing brain hemorrhage (arrowhead) at 52 hpf, and quantification (N=3, n=194 embryos). (D-F) Dorsal images of wildtype (D) and *nkx3.1*$^{-/-}$ (E) expressing *Tg(pdgfrβ:GFP)* and *Tg(kdrl:mCherry*) show fewer brain pericytes in mutants at 75 hpf (F, n=17 hets and 23 mutants). (G-I) Nkx3.1 gain-of-function (GOF, *Tg(hsp70l:tBFP-2a-nkx3.1))* show more pericytes (arrowheads) as compared to control embryos *(Tg(hsp70l:tBFP,* n=20 control and 19 GOF*))*. Statistical significance was calculated using the Student's t-test. Scale bar is 50μm.

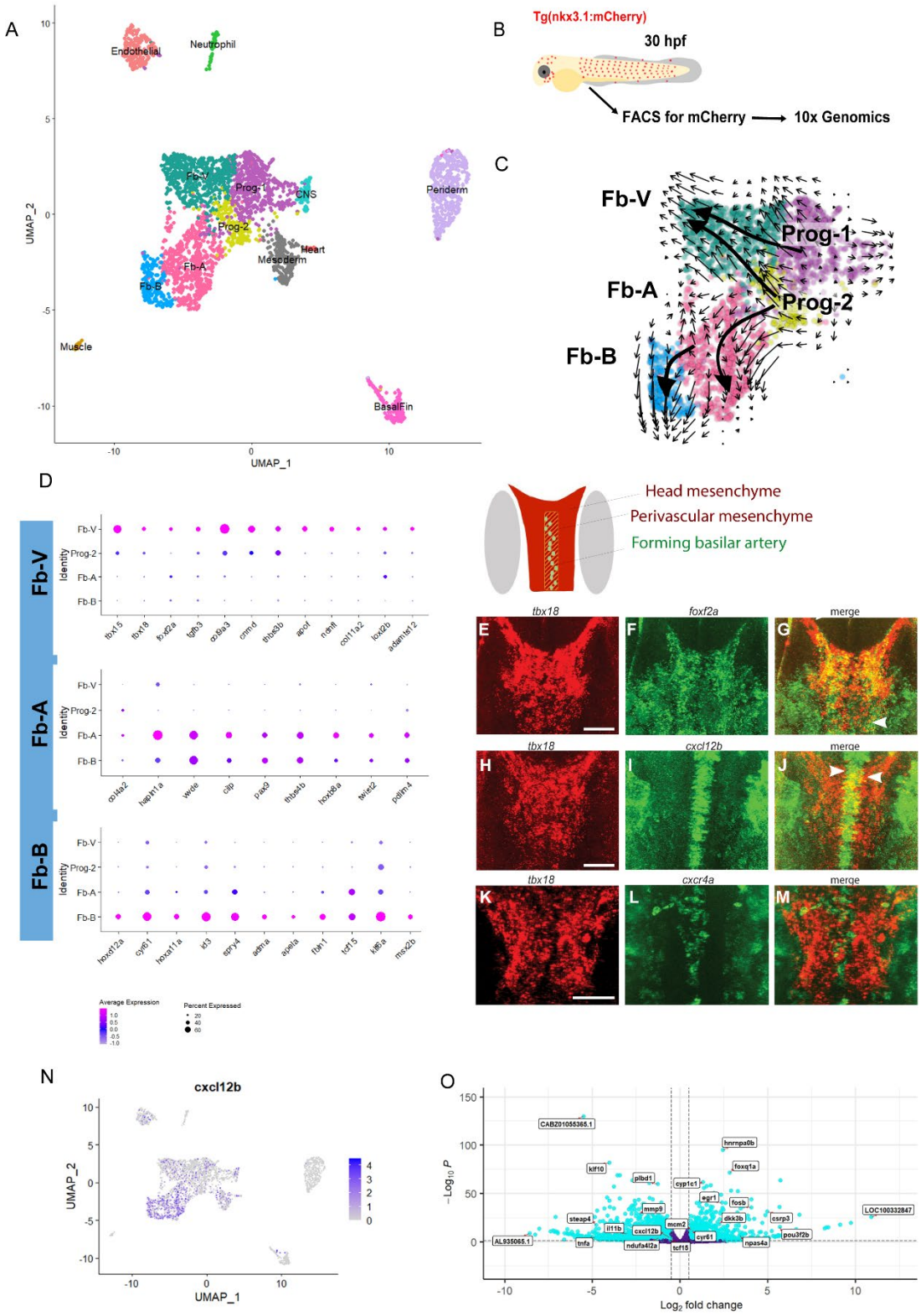

Fig. 3: Next generation sequencing analysis of *nkx3.1*$^{NTR\text{-}mcherry}$ and *nkx3.1*$^{-/-}$ embryos at 30 hpf. (A) Single cell clusters of *nkx3.1*$^{NTR\text{-}mcherry}$ embryos at 30 hpf. (B) Schematic showing workflow for single cell sequencing of *nkx3.1*$^{NTR\text{-}mcherry}$ cells. (C) RNA-velocity analysis of subclustered *nkx3.1*$^{NTR\text{-}mcherry}$ cells of the Progenitor and FB-V, FB-A, and Fb-B clusters. (D) Dot plots showing key marker genes of FB-V, FB-A, and Fb-B clusters. (E-M) HCR expression analysis of Fb-V genes at 36 hpf with the schematic showing relative locations of the ventral head mesenchyme and the forming basilar artery. (E-G) *tbx18* (red) and *foxf2a* (green) show expression overlap at 36 hpf in the ventral head (yellow, arrowheads). (H-J) *tbx18* (red) and *cxcl12b* (green) show expression overlap at 36 hpf in the ventral head (yellow, arrowheads). (K-M) *tbx18* (red) is expressed in the perivascular space surrounding the *cxcr4a* (green) expressing basilar artery in the ventral head at 36 hpf. (N) *cxcl12b* feature plot showing its expression across clusters including Fb-V. (O) Bulk sequencing volcano plot of *nkx3.1*$^{-/-}$ embryos at 30 hpf. Scale bar is 50μm.

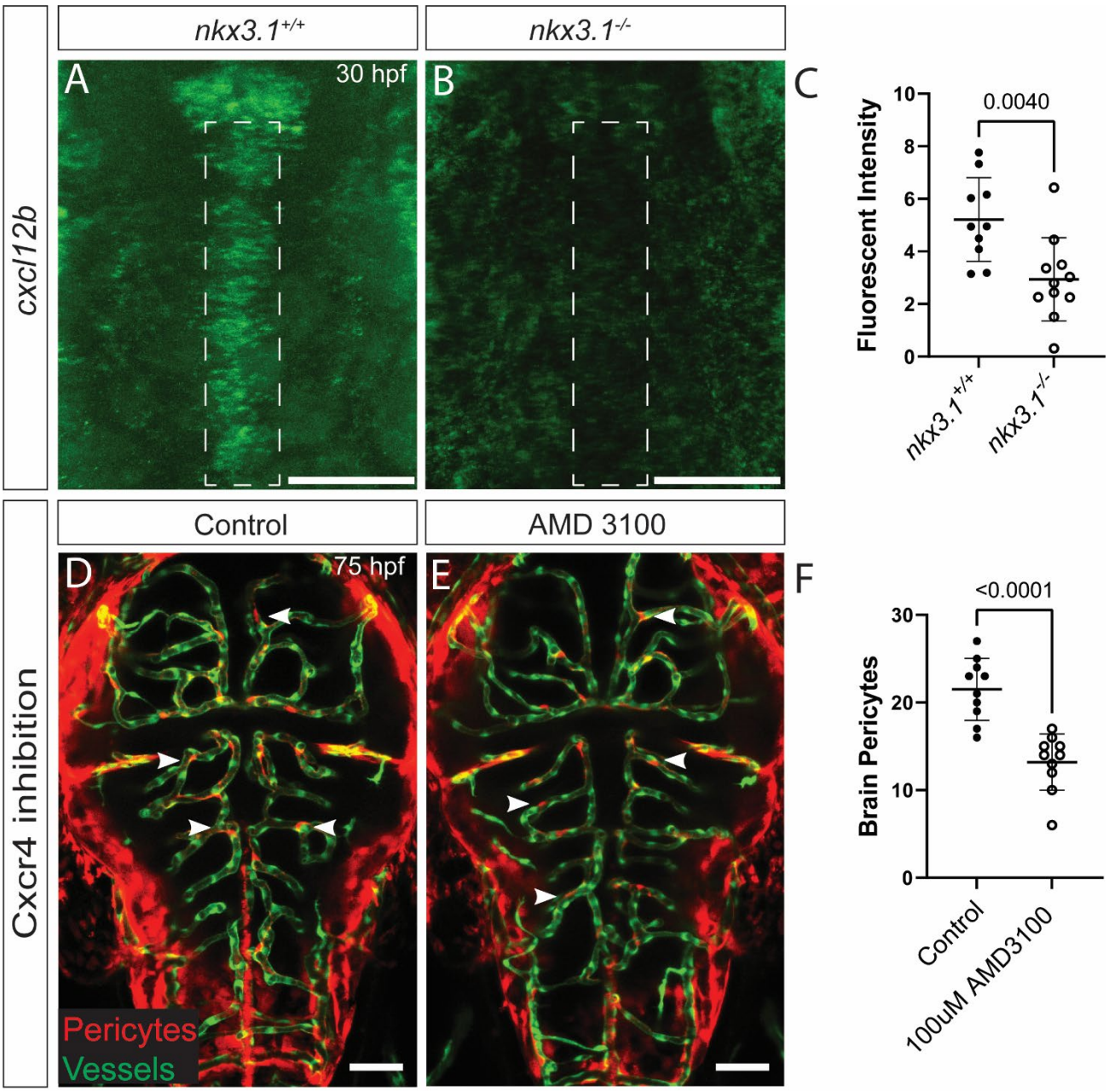

Fig. 4: *cxcl12b* is regulated by *nkx3.1*; loss of Cxcr4 signaling reduces brain pericytes. All embryos were imaged dorsally in the head region. (A-B) *cxcl12b* mRNA expression is reduced in the embryonic head of *nkx3.1*$^{-/-}$ mutants at 30 hpf. (C) Fluorescent intensity quantification of regions marked by dotted lines in A and B, n=10. (D-F) Inhibition of Cxcr4 from 24-75 hpf using AMD 3100 leads to reduced brain pericyte (arrowheads) numbers at 75 hpf (n=10). Pericytes (red) are labeled by *TgBAC(pdgfrβ:Gal4)* and *Tg(UAS:NTR-mCherry)*. Brain vessels (green) in D and E are labeled by *Tg(flk:GFP)*. Statistical significance was calculated using the Student's t-test. Scale bar is 50μm.

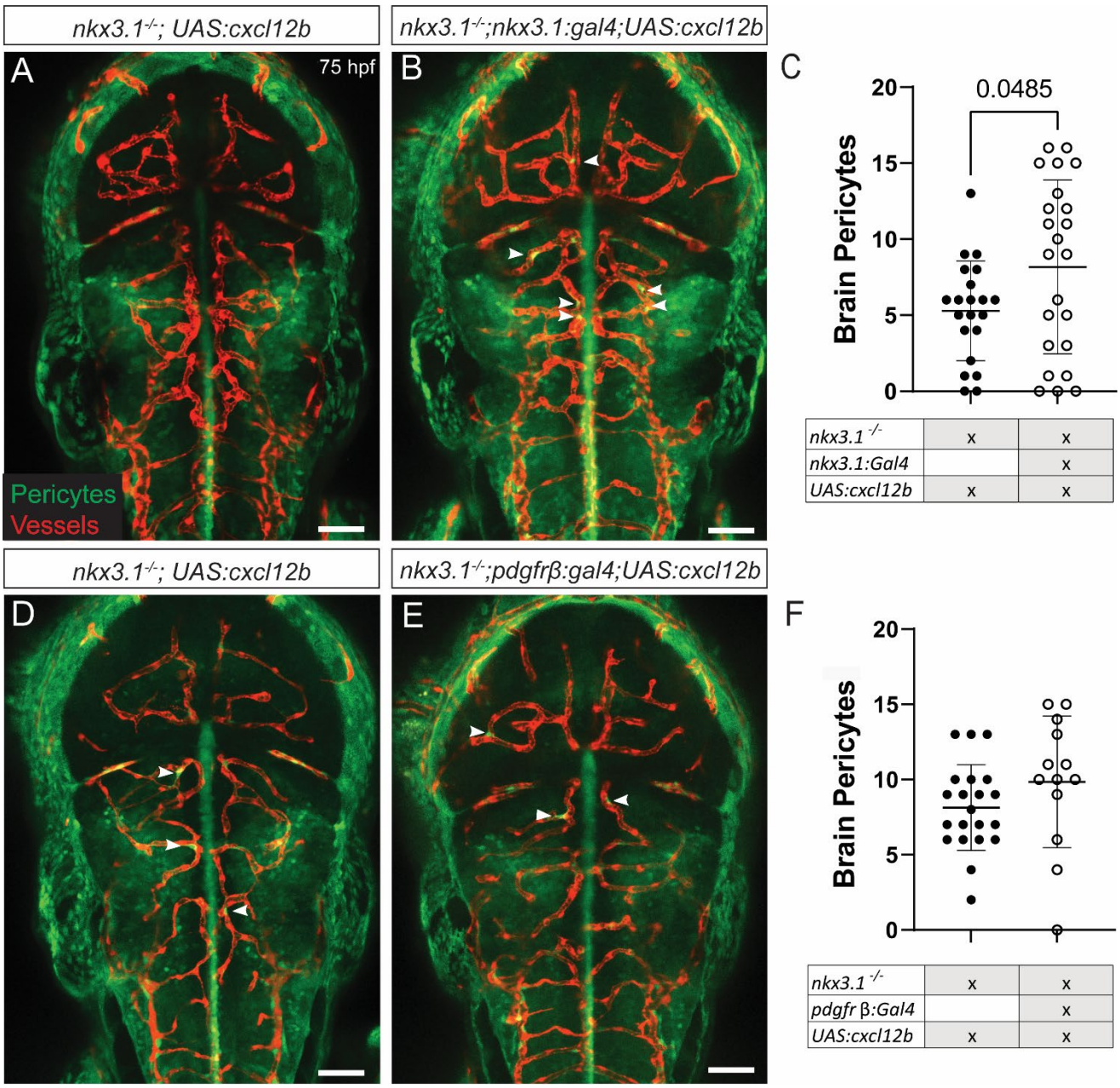

Fig. 5: Re-expression of Cxcl12b rescues pericyte numbers in *nkx3.1*$^{-/-}$. All embryos were imaged dorsally in the head region. (A-C) Genetic rescue expressing *cxcl12b* under the *nkx3.1* driver *TgBAC(nkx3.1:Gal4)* rescues pericyte numbers at 75 hpf. (D-F) Genetic rescue expressing *cxcl12b* under the *pdgfrβ* driver *TgBAC(pdgfrβ:Gal4)* does not rescue pericyte numbers at 75 hpf. Arrowheads mark brain pericytes (green) labeled by *TgBAC(pdgfrβ:GFP)* and brain vessels (red) are llabeled by *Tg(kdrl:mCherry)*. Statistical significance was calculated using the Student's t-test. Scale bar is 50μm.

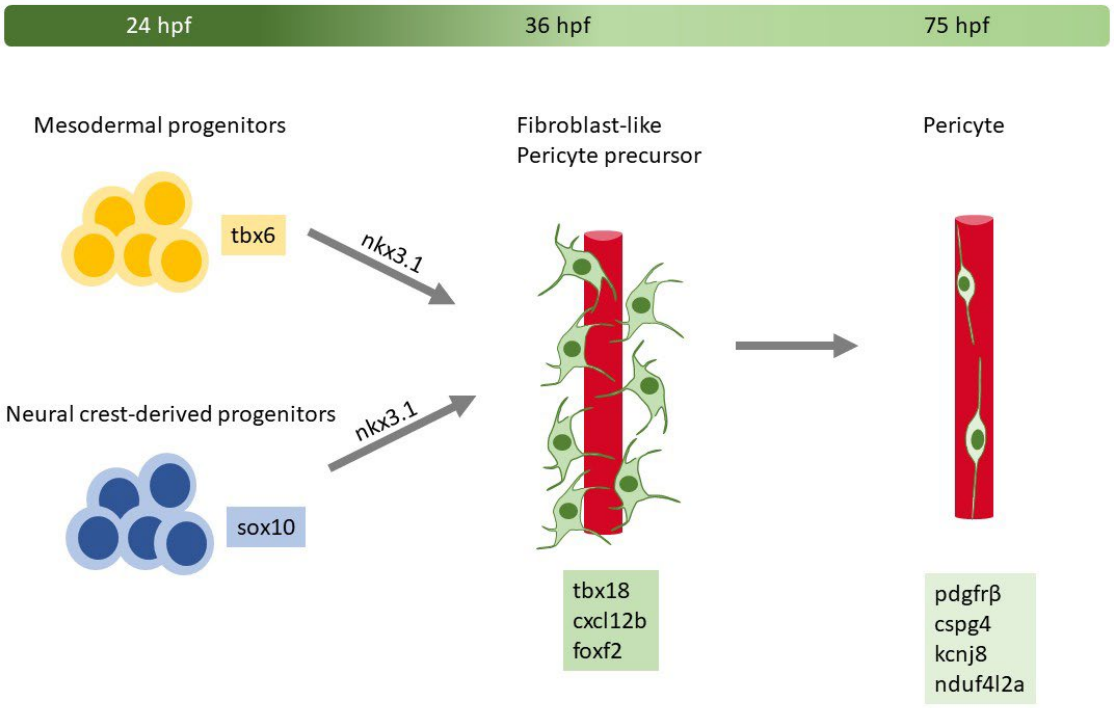

Fig. 6: nkx3.1 is essential in pericyte precursors

Model of cell types and genes leading to pericyte differentiation. Both mesodermal and neural crest progenitors differentiate into nkx3.1 expressing precursors that differentiate into mature perictyes.